

# DEVELOPMENT OF A REAL-TIME WAVEFORM MONITORING SYSTEM FOR PULSED POWER SUPPLIES AT TAIWAN PHOTON SOURCE

W. Y. Lin\*, H. J. Tsai, T. W. Hsu, T. Y. Lee, C. Y. Hung, B. Y. Huang  
National Synchrotron Radiation Research Center, NSRRC, Hsinchu, Taiwan

## Abstract

A real-time waveform monitoring system has been developed for the pulsed power supplies in the injection chain of the Taiwan Photon Source (TPS). The system covers eight kicker and septum magnets spanning the Booster Ring and Storage Ring injection path. Two operational incidents involving SR Injection Septum 1 motivated its development: in both cases, waveform anomalies that were imperceptible by visual inspection led to severe injection efficiency degradation or complete injection failure. The system acquires waveforms via EPICS Channel Access, computes shot-averaged deviations from a stored reference, and compares them against physics-motivated alarm thresholds derived from dedicated machine study experiments. The thresholds are expressed as time-resolved curves that directly map waveform error to injection efficiency degradation. The system has been deployed and is currently in operation at TPS.

## INTRODUCTION

The Taiwan Photon Source (TPS) is a 3 GeV third-generation synchrotron light source operated by the National Synchrotron Radiation Research Center (NSRRC) in top-up mode to maintain a stable stored current [1]. The injection chain consists of a Booster Ring (BR) and a Storage Ring (SR) connected in series, and the waveform quality of pulsed power supplies — kicker and septum magnets — directly determines injection efficiency and beam stability.

Two separate incidents involving SR Injection Septum 1 motivated this work. The first occurred on June 25, 2025: injection into the storage ring was completely lost despite normal BTS transport, and post-incident investigation revealed a waveform deviation so subtle that it was virtually indistinguishable by visual inspection (Fig. 1b) — a peak amplitude deviation of only a few percent was sufficient to cause complete injection failure. The second occurred on July 17, 2025, when unstable septum output caused injection efficiency to fluctuate severely and repeatedly drop toward zero (Fig. 1a). Both incidents highlighted a fundamental limitation of conventional operator monitoring, motivating the development of an automated system capable of detecting subtle waveform deviations quantitatively before injection performance degrades.

## MONITORING SYSTEM DESIGN

### Monitored Devices

The system monitors eight pulsed power supply devices covering the complete injection path from the BR injection

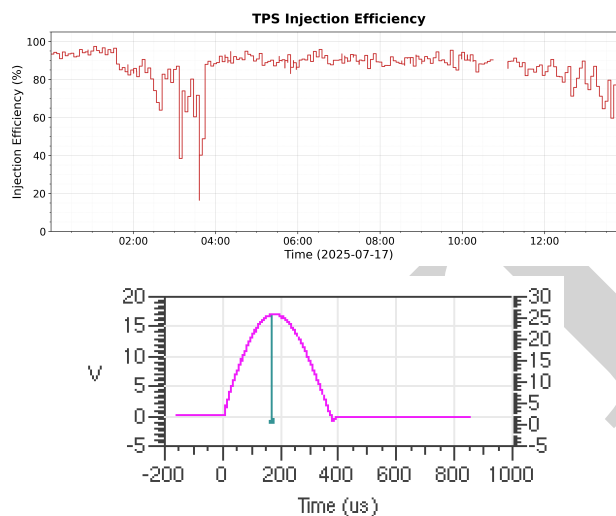


Figure 1: Operational incidents motivating this work. (a) Injection efficiency recorded on July 17, 2025, showing severe fluctuation due to unstable SR Injection Septum 1 output. (b) SR Injection Septum 1 waveform as displayed on the operator console. A peak amplitude deviation of only a few percent — imperceptible at this display scale — is sufficient to cause complete injection failure, as experienced on June 25, 2025.

point to the SR injection point. All eight devices operate at a nominal injection efficiency of approximately 84%, measured independently for each device during the machine study experiments.

### Software Architecture

The system is implemented in Python and acquires waveform data via EPICS Channel Access [2]. After each injection trigger, a background thread accumulates 30 consecutive waveforms and computes their average for comparison against a stored reference. The graphical interface is built with Qt and provides three views: a *Status Overview* showing real-time Mean Diff, Max Diff, and alarm status for all eight devices (Fig. 2, top); a *Waveform View* displaying the averaged waveform overlaid with the reference and the difference curve with three threshold lines (Fig. 2, bottom); and an *Alarm Log* with timestamped records exportable as CSV.

### Reference Waveform and Monitor Window

At startup or on operator request, the system presents a dialog allowing the operator to either capture 30 consecutive shots as a fresh reference or load a previously saved reference from file. The monitor window and difference metrics are defined according to device type.

\* lin.lucien@nsrrc.org.tw

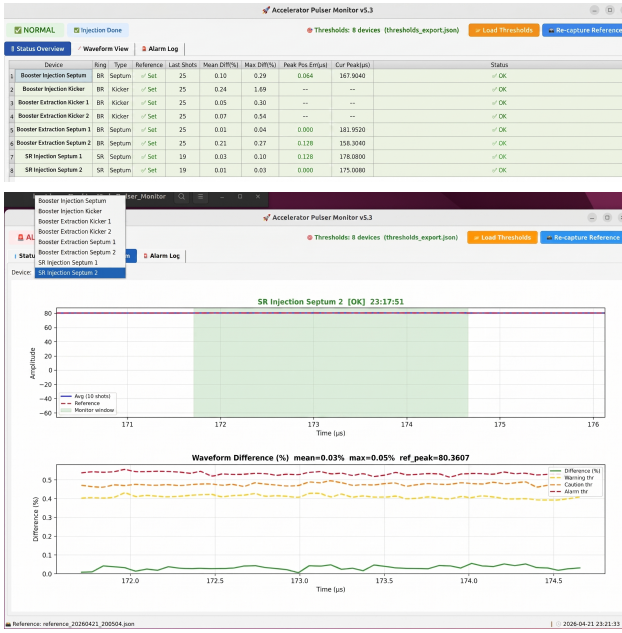


Figure 2: Graphical user interface of the monitoring system. (Top) Status Overview showing real-time Mean Diff, Max Diff, and peak position error for all eight devices, with all channels reporting normal status. (Bottom) Waveform View for SR Injection Septum 2, showing the 30-shot averaged waveform (blue), reference (red dashed), monitor window (green shaded), and the difference curve with Warning (yellow), Caution (orange), and Alarm (red) threshold lines.

**Septum devices.** The peak center of the reference waveform is computed using a threshold-crossing method: all samples exceeding 95% of the peak amplitude are identified, and the midpoint of the resulting interval is taken as the peak center. This approach is robust against noise-induced jitter and ensures that the reference and all subsequent real-time acquisitions share a common time-axis origin, eliminating systematic offsets that would otherwise arise from timing differences between machine study and real-time operation. A fixed-width monitor window of  $\pm 1.5 \mu\text{s}$  around the reference peak center (total width  $3.0 \mu\text{s}$ ) is applied, ensuring the comparison region always aligns with the most sensitive portion of the waveform. Within this window, the point-wise difference  $D(t)$  defined in Eq. (1) is computed to derive Mean Diff and Max Diff. In addition, a peak position error is computed as the absolute shift of the current waveform peak center relative to the reference. While  $D(t)$  is sensitive to overall amplitude deviations, its response to a pure timing shift is limited: when the trigger timing of a septum drifts, the waveform shape may remain intact yet  $D(t)$  fails to reflect the anomaly effectively. The peak position error therefore serves as an independent timing monitor dedicated to detecting such events. A shift exceeding  $2.0 \mu\text{s}$  issues a Warning; a shift exceeding  $4.0 \mu\text{s}$  issues an Alarm.

**Kicker devices.** The window end point is fixed at a pre-configured time boundary; the window start is determined dynamically by locating the first point at which the reference waveform reaches 80% of its peak amplitude (Flat-top Start),

excluding the rising edge and eliminating false alarms from timing jitter. The two Booster Extraction Kickers (BEK1 and BEK2) share the same window end at  $6.5 \mu\text{s}$  with a mutual delay separation of  $192 \text{ ns}$ . The Booster Injection Kicker (BIK) requires special treatment: its waveform contains two temporally separated flat-top segments corresponding to successive beam turns in the booster ring, separated by the revolution period  $T = 1.656 \mu\text{s}$ . A single window would be dominated by the inter-pulse valley; the system therefore applies independent windows to each segment — Segment 1 covering  $6.0\text{--}6.9 \mu\text{s}$  and Segment 2 covering  $7.6\text{--}8.5 \mu\text{s}$  — with Mean Diff and Max Diff computed separately, raising an alarm if either segment exceeds its threshold.

### Waveform Difference Metric

Within the monitor window, the point-wise deviation between the current averaged waveform  $V(t)$  and the reference  $V_{\text{ref}}(t)$  is normalised to the peak amplitude of the reference waveform within the monitor window,  $V_{\text{peak,ref}}$ :

$$D(t) = \frac{|V(t) - V_{\text{ref}}(t)|}{V_{\text{peak,ref}}} \times 100\%. \quad (1)$$

Two scalar statistics are derived: Mean Diff, the time-averaged value of  $D(t)$  over the window, which reflects the overall waveform deviation; and Max Diff, the maximum value, which captures localised transient anomalies. For septum-type devices, the additional peak position error is computed as described above.

## MACHINE STUDY AND THRESHOLD DERIVATION

### Experimental Method and Characteristic Behaviours

To establish a quantitative mapping between waveform error and injection efficiency degradation, dedicated machine study experiments were performed for each device. With the machine in stable operation, the HV setting was scanned systematically; at each setpoint, 50-shot averages of injection efficiency (mean  $\pm 1\sigma$ ) and the waveform error distribution were recorded simultaneously, yielding a complete *waveform error*  $\rightarrow$  *injection efficiency* calibration curve (Fig. 3). Two distinct behaviours were observed: kicker-type devices exhibit an efficiency saturation plateau near the nominal operating point followed by a sharp drop below a critical HV threshold; septum-type devices show a smoother, monotonic efficiency curve with small shot-to-shot variance throughout, confirming stable and well-characterised behaviour.

### Three-Curve Threshold Derivation

From the calibration data, three efficiency target levels are defined relative to each device's baseline:  $-5\%$  (Warning),  $-10\%$  (Caution), and  $-15\%$  (Alarm). At each target level, the HV setpoint corresponding to that efficiency drop is identified by interpolation, and the waveform difference curve  $D(t)$  recorded at that setpoint is extracted. The mean  $\mu(t)$

and standard deviation  $\sigma(t)$  of  $D(t)$  at each level are then computed point-wise. Three independent threshold curves are produced, one per level, as defined in Table 1.

Table 1: Alarm Threshold Curve Definitions

Curve	Colour	Definition
Warning	Yellow	$\mu(t) + 2\sigma(t)$ at $-5\%$ level
Caution	Orange	$\mu(t) + 2\sigma(t)$ at $-10\%$ level
Alarm	Red	$\mu(t) + 2\sigma(t)$ at $-15\%$ level

Each threshold equals the mean waveform error plus two standard deviations at the corresponding efficiency-drop level, representing the boundary beyond which the observed deviation is statistically inconsistent with normal operation at that degradation level. The three curves provide graduated sensitivity: the Warning curve responds to early-stage degradation ( $-5\%$ ), while the Alarm curve is reserved for severe anomalies ( $-15\%$ ), directly corresponding to the machine study operating points.

### Time-Resolved Threshold Curves

The thresholds are expressed as *time-resolved curves* rather than single scalar values (Fig. 4), reflecting the fact that different portions of the waveform have different sensitivities to injection efficiency. For septa, the flat top is highly uniform and all three thresholds remain nearly constant across the entire monitor window — for SR Injection Septum 2, the Warning threshold is  $\sim 0.4\%$ , Caution  $\sim 0.5\%$ , and Alarm  $\sim 0.55\%$  — a sensitivity level specifically designed to detect the kind of imperceptible anomaly that caused the June 2025 incident.

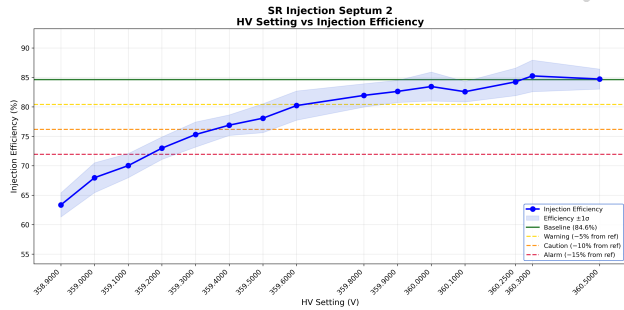


Figure 3: HV scan result for SR Injection Septum 2 (baseline efficiency: 84.6%). The efficiency increases monotonically from  $\sim 63\%$  to  $\sim 85\%$  as the HV setting is raised, with small shot-to-shot variance throughout. The three dashed horizontal lines indicate the Warning ( $-5\%$ ), Caution ( $-10\%$ ), and Alarm ( $-15\%$ ) efficiency target levels used for threshold derivation.

### CONCLUSION

A real-time waveform monitoring system for pulsed power supplies has been developed and deployed at TPS. The sys-

tem was motivated by two operational incidents in which waveform anomalies imperceptible to visual inspection caused severe injection degradation or complete injection

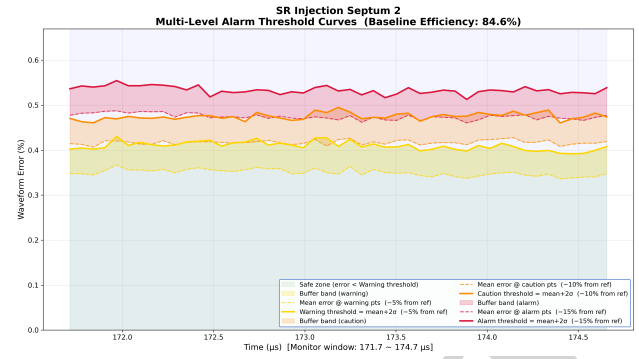


Figure 4: Time-resolved alarm threshold curves for SR Injection Septum 2 (baseline efficiency: 84.6%). The Warning (yellow), Caution (orange), and Alarm (red) thresholds remain nearly constant across the entire monitor window at  $\sim 0.4\%$ ,  $\sim 0.5\%$ , and  $\sim 0.55\%$  respectively — a sensitivity level designed to detect waveform deviations imperceptible by visual inspection. The green shaded area indicates the safe zone below the Warning threshold.

tem was motivated by two operational incidents in which waveform anomalies imperceptible to visual inspection caused severe injection degradation or complete injection failure. Through dedicated machine study experiments, three physics-motivated alarm threshold curves — Warning, Caution, and Alarm — were derived independently for each device, each defined as  $\mu(t) + 2\sigma(t)$  of the waveform error at the corresponding efficiency-drop level ( $-5\%$ ,  $-10\%$ ,  $-15\%$ ). For septum-type devices, the Warning threshold is as low as  $\sim 0.4\%$ , enabling detection of deviations far below the limit of visual inspection. The Booster Injection Kicker is monitored with independent dual-segment windows to handle its double-pulse waveform structure. A threshold-crossing peak center alignment procedure ensures the reference waveform shares a common time-axis origin with all real-time acquisitions, eliminating false alarms due to systematic timing offsets. The system is currently in operation at TPS and will continue to accumulate data to evaluate alarm performance and support predictive maintenance.

### REFERENCES

- [1] C. C. Kuo *et al.*, “Commissioning of the Taiwan Photon Source”, in *Proc. IPAC'15*, Richmond, VA, USA, May 2015, pp. 1314–1316. doi:10.18429/JACoW-IPAC2015-TUXC3
- [2] L. R. Dalesio *et al.*, “The Experimental Physics and Industrial Control System architecture: Past, present, and future”, *Nucl. Instrum. Methods Phys. Res. A*, vol. 352, pp. 179–184, 1994. doi:10.1016/0168-9002(94)91493-1